ETSI TR 103 297 V1.1.1 (2017-07)

Satellite Earth Stations and Systems (SES);
SC-FDMA based radio waveform technology
for Ku/Ka band satellite service

Reference
DTR/SES-00366

Keywords
air interface, FDMA, satellite, wideband

ETSI

650 Route des Lucioles
F-06921 Sophia Antipolis Cedex - FRANCE

Tel.: +33 4 92 94 42 00 Fax: +33 4 93 65 47 16

Siret N° 348 623 562 00017 - NAF 742 C
Association à but non lucratif enregistrée à la
Sous-Préfecture de Grasse (06) N° 7803/88

Contents

Intellectual Property Rights

Essential patents

IPRs essential or potentially essential to the present document may have been declared to ETSI. The information pertaining to these essential IPRs, if any, is publicly available for **ETSI members and non-members**, and can be found in ETSI SR 000 314: *"Intellectual Property Rights (IPRs); Essential, or potentially Essential, IPRs notified to ETSI in respect of ETSI standards"*, which is available from the ETSI Secretariat. Latest updates are available on the ETSI Web server (https://ipr.etsi.org/).

Pursuant to the ETSI IPR Policy, no investigation, including IPR searches, has been carried out by ETSI. No guarantee can be given as to the existence of other IPRs not referenced in ETSI SR 000 314 (or the updates on the ETSI Web server) which are, or may be, or may become, essential to the present document.

Trademarks

The present document may include trademarks and/or tradenames which are asserted and/or registered by their owners. ETSI claims no ownership of these except for any which are indicated as being the property of ETSI, and conveys no right to use or reproduce any trademark and/or tradename. Mention of those trademarks in the present document does not constitute an endorsement by ETSI of products, services or organizations associated with those trademarks.

Foreword

This Technical Report (TR) has been produced by ETSI Technical Committee Satellite Earth Stations and Systems (SES).

Modal verbs terminology

In the present document "**should**", "**should not**", "**may**", "**need not**", "**will**", "**will not**", "**can**" and "**cannot**" are to be interpreted as described in clause 3.2 of the ETSI Drafting Rules (Verbal forms for the expression of provisions).

"**must**" and "**must not**" are **NOT** allowed in ETSI deliverables except when used in direct citation.

1 Scope

The present document aims at assessing the performance of a SC-FDMA-based radio waveform over geostationary satellites in Ku/Ka band. Moreover, it aims at defining an evaluation framework for performance comparison with existing waveform technologies (e.g. DVB-S2, DVB-S2X and DVB-RCS2), focusing on the radio and physical layers.

The present document deals with satellite return link only. The forward link is for further study. For the return link, two use cases have been identified and treated so far, Satellite News Gathering (DSNG) and Broadband Access.

The present document provides a description of the waveforms to be compared; it identifies their key characteristics, defines the system model used for comparison and presents comparative performance results in terms of spectral efficiency. A complexity analysis is also performed.

2 References

2.1 Normative references

Normative references are not applicable in the present document.

2.2 Informative references

References are either specific (identified by date of publication and/or edition number or version number) or non-specific. For specific references, only the cited version applies. For non-specific references, the latest version of the referenced document (including any amendments) applies.

NOTE: While any hyperlinks included in this clause were valid at the time of publication, ETSI cannot guarantee their long term validity.

The following referenced documents are not necessary for the application of the present document but they assist the user with regard to a particular subject area.

[i.1] ETSI EN 302 307: "Digital Video Broadcasting (DVB); Second generation framing structure, channel coding and modulation systems for Broadcasting, Interactive Services, News Gathering and other broadband satellite applications (DVB-S2)".

[i.2] DVB Document A83-2: "Digital video broadcasting (DVB); Second generation framing structure, channel coding and modulation systems for broadcasting, interactive services, news gathering and other broad-band satellite applications, Part II: S2-Extensions (DVB-S2X)-(Optional)", March 2014.

[i.3] ETSI TS 136 211 (V8.3.0): "LTE; Evolved Universal Terrestrial Radio Access (E-UTRA); Physical channels and modulation (3GPP TS 36.211 version 8.3.0 Release 8)".

[i.4] DVB BlueBook A160: "Digital Video Broadcasting (DVB); Next Generation broadcasting system to Handheld, physical layer specification (DVB-NGH)".

[i.5] Ciochina-Duchesne C., Castelain D., Bouttier A.: "Satellite profile in DVB-NGH," Advanced Satellite Multimedia Systems Conference (ASMS) and 12th Signal Processing for Space Communications Workshop (SPSC), Baiona, Spain, 5-7 September 2012.

[i.6] DVB Document A162: "Guidelines for Implementation and Use of LLS: ETSI EN 301 545-2", February 2013.

[i.7] Recommendation ITU-R M.2047-0 (12-2013): "Detailed specifications of the satellite radio interfaces of International Mobile Telecommunications-Advanced (IMT Advanced)".

[i.8] C. Ciochina: "Physical layer design for the uplink of mobile cellular radiocommunications systems", PhD defence, July 2009.

[i.9] Okuyama S., Takeda K., Adachi F.: "MMSE Frequency-Domain Equalization Using Spectrum Combining for Nyquist Filtered Broadband Single-Carrier Transmission," Vehicular Technology Conference (VTC 2010-Spring), 16-19 May 2010.

[i.10] ETSI TR 102 376 (V1.1.1) (02-2005): "Digital Video Broadcasting (DVB); User guidelines for the second generation system for Broadcasting, Interactive Services, News Gathering and other broadband satellite applications (DVB-S2)".

[i.11] ETSI TR 102 376-2 (V1.1.1) (November 2015): "Digital Video Broadcasting (DVB); Implementation guidelines for the second generation system for Broadcasting, Interactive Services, News Gathering and other broadband satellite applications; Part 2: S2 Extensions (DVB-S2X)".

[i.12] M. Morelli, C.-C. J. Kuo and M.-O. Pun: "Synchronization Techniques for Orthogonal Frequency Division Multiple Access (OFDMA): A Tutorial Review", Proceedings of the IEEE, vol. 95, no. 7, pp. 1394- 1427, July 2007.

[i.13] ETSI TS 136 213: "LTE; Evolved Universal Terrestrial Radio Access (E-UTRA); Physical layer procedures (3GPP TS 36.213 Release 11)".

[i.14] D. Chu: "Polyphase Codes with Good Periodic Correlation Properties," IEEE Transactions on Information Theory, vol. 18, no. 4, pp. 531-532, July 1972.

[i.15] Y. Wen, W. Huang and Z. Zhang: "CAZAC sequence and its Application in LTE Random Access", In Proceedings of IEEE Information Theory Workshop, October 2006, pp. 544-547.

[i.16] F. Rossetto and M. Berioli: "On synchronisation for SC-FDMA waveform over geo satellite networks" in Advanced Satellite Multimedia Systems Conference (ASMS) and 12th Signal Processing for Space Communications Workshop (SPSC), 2012 6th, September 2012, pp. 233-237.

[i.17] U. Mengali and M. Morelli: "Data-aided frequency estimation for burst digital transmission" Communications, IEEE Transactions on, vol. 45, no. 1, pp. 23-25, January 1997.

[i.18] P. H. Moose: "A technique for orthogonal frequency division multiplex- ing frequency offset correction," Communications, IEEE Transactions on, vol. 42, no. 10, pp. 2908-2914, October 1994.

[i.19] Global Positioning System Standard Positioning Service Performance Standard, 4th edition, September 2008.

[i.20] B. M. Popović: "Efficient Matched Filter for the Generalized Chirp-Like Polyphase Sequences" IEEE Transactions on Aerospace and Electronic Systems, Vol. 30, No. 3, pp. 769-777, July 1994.

[i.21] Panasonic: "R1-071517: RACH Sequence Allocation for Efficient Matched Filter Implementation", www.3gpp.org, 3GPP TSG RAN WG1, meeting 48bis, St Julians, Malta, March 2007.

[i.22] D. Castelain, C. Ciochina-Duchesne, J. Guillet and F. Hasegawa: "SC-OFDM, a Low-Complexity Technique for High Performance Satellite Communications", ICSSC"2014, San Diego, August 2014.

3 Symbols and abbreviations

3.1 Symbols

For the purposes of the present document, the following symbols apply:

α	Roll-off factor
M	DFT precoding size
N	IDFT size
Ncar	Number of carriers per transponder
N_{CP}	CP length
N_{guard}	Number of guard subcarriers
N_{taps}	Number of taps for the finite impulse response filter
ovs	Oversampling factor
ρ	Code rate
Rs	Symbol rate (baud)

3.2 Abbreviations

For the purposes of the present document, the following abbreviations apply:

3GPP	Third Generation Partnership Project
AM/AM	Amplitude Modulation/Amplitude Modulation
AM/PM	Amplitude Modulation/Phase Modulation
APSK	Amplitude Phase Shift Keying
AWGN	Additive White Gaussian Noise
BER	Bit-Error Ratio
BICM	Bit Interleaved Coded Modulation symbols
CAZAC	Constant Amplitude Zero AutoCorrelation
CCDF	Complementary Cumulative Distribution Function
CFO	Carrier Frequency Offset
CP	Cyclic Prefix
DFT	Discrete Fourier Transform
DL	DownLink
DSNG	Digital Satellite News Gathering
DVB	Digital Video Broadcasting
DVB-NGH	DVB New Generation Handheld
DVB-RCS	DVB Return Channel via Satellite
DVB-S	Digital Video Broadcasting via Satellite
FDE	Frequency Domain Equalization
FDMA	Frequency Division Multiple Access
FDT	Frequency Domain Transmitter
FFT	Fast Fourier Transform
FIR	Finite Impulse Response
GEO	Geostationary Orbit
GPS	Global Positioning System
GT	Guard Time
HPA	High Power Amplifier
IBO	Input Back-Off
ICI	Inter-Carrier Interference
IDFT	Inverse Discrete Fourier Transform
IMI	Inter-Modulation Interference
IMT	International Mobile Telecommunications
IMUX	Input MUltipleXer filter
ISI	Inter-Symbol Interference
INP	Instantaneous Normalized Power
ITU-R	International Telecommunication Union-Radiocommunications sector
LTE	Long Term Evolution
MAI	Multiple Access Interference
MLE	Maximum Likelihood Estimator

MODCOD	Modulation & Coding
MSE	Mean-Squared Error
NC	Not Compensated
NCC	Network Control Centre
NR	New Radio
OFDM	Orthogonal Frequency Division Multiplex
PAPR	Peak to Average Power Ratio
PER	Packet Error Rate
PN	Phase Noise
PRACH	Physical Random Access CHannel
PSK	Phase Shift Keying
OBO	Output Back-Off
OFDMA	Orthogonal Frequency Division Multiple Access
OMUX	Output Multiplexer Filter
QAM	Quadrature Amplitude Modulation
QPSK	Quaternary Phase Shift Keying
RA	Random Access
RACH	Random Access Channel
RCST	Return Channel Satellite Terminal
RF	Radio Frequency
RTT	Round Trip Time
SC	Single Carrier
SC-FDMA	Single Carrier-Frequency Division Multiple Access
SC-OFDM	Single Carrier-Orthogonal Frequency Division Multiplexing
SC-TDM	Single Carrier-Time Division Multiplexing
SE	Spectral Efficiency
SIR	Signal-to-Interference Ratio
SNG	Satellite News Gathering
SNR	Signal-to-Noise Ratio
SRRCF	Square Root Raised Cosine Filter
SSPA	Solid State Power Amplifier
TD	Total Degradation
TDE	Time Domain Equalization
TDM	Time Division Multiplexing
TDMA	Time Division Multiple Access
TDT	Time Domain Transmitter
TE	Timing Error
TWT	Travelling Wave Tube
TWTA	Travelling Wave Tube Amplifier
UE	User Equipment
UL	Uplink
ZC	Zadoff-Chu

4 Introduction

The return link in satellite may correspond to different use cases.

The present document evaluates the performance of SC-FDMA radio interface for satellite broadband systems operating in Ku or Ka band, focusing on the physical layer.

The presentdocument deals with satellite return link only. The forward link part is for further study. For the return link, two use cases have been identified and treated so far, DSNG and Broadband access.

5 Return link

5.1 Introduction

The return link in satellite may correspond to different use cases.

The first use case that is described and simulated in the present document is a professional return link use case, in practice a typical DSNG use case. Different relatively wide-band SC-OFDM signals (i.e. SC-FDMA with full subcarrier allocation) are transmitted to the satellite by a few transmitters in the same band. The multiple access scheme is thus FDMA and not SC-FDMA. These signals are not assumed synchronized neither in time nor in frequency, which implies that a slight frequency guard band is sometimes needed, depending on the robustness of the modulation. This use case is the same as the return link professional one considered in DVB-S2x [i.2]. This DSNG use case is illustrated in Figure 1.

Broadband access (DVB-RCS2) corresponds to another important return link use case. This use case is similar to LTE uplink, where the different signals (not as wideband as in previous case), with SC-FDMA multiple access, are assumed synchronized in time and frequency, which implies new constraints for insuring this synchronization. The number of signals simultaneously transmitted in the same band is much higher than in the previous use case, which explains the choice of the SC-FDMA multiple access scheme for obtaining a good efficiency. In this use case, the cyclic prefix [i.4], [i.5] and [i.9] is used to relax the constraints on the synchronization, which means that its size are dimensioned for this purpose. However and contrary to the DSNG use case, a frequency guard band is generally not necessary. This broadband access use case is illustrated in Figure 1.

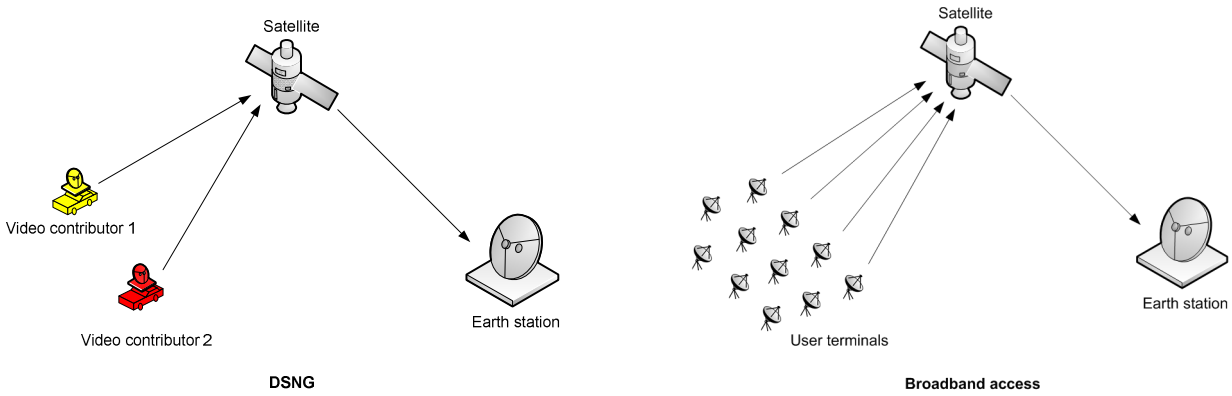

Figure 1: Return link use cases

Table 1: Return link use cases

	DSNG use case	Broadband access use case
Radio resource assigned per terminal	One or several full SC-FDMA carrier(s)	Several sub-carriers of a SC-FDMA carrier
Operational constraints	No need for synchronization between satellite terminals	Need for synchronization between satellite terminals
Multiple access scheme	FDMA type: Single terminal per SC-FDMA carrier	SC-FDMA: Several terminals per SC-FDMA carrier
Comparison with existing waveform technologies	DVB-S2x	DVB-RCS2

In particular, the present document compares the performances for the return link of two types of radio interface:

- SC-TDM: this refers to current satellite communication standards such as DVB-S2 [i.1] and DVB-S2X [i.2]. It corresponds to single carrier sequential transmission of modulation signals, with a spectrum shaped by a root-raised cosine filter with different roll-off factors α. It was designed for satellite communications to maximize the efficiency of HPA on-board satellite by minimizing the envelope variation of the signal and then limiting the non-linear effects.

- SC-FDMA is a transmission technique derived from OFDMA via DFT precoding. SC-FDMA is exhibiting low envelope variations and is having a natural compatibility with zero roll-off. As is the case for OFDMA and all its precoded counterparts, SC-FDMA allows low complexity per-subcarrier equalization in the frequency domain. In its full spectral allocation version, SC-FDMA is also coined SC-OFDM [i.22].
  In the present document, the performance of the access scheme is not taken into account. Hence, the performance of both SC-TDM and SC-FDMA waveform signals are compared by applying the same access scheme to the spectrum.

The differences between the different signal types are illustrated in Table 2.

Table 2: The analysed signals

	SC-FDMA	SC-TDM = TDM	SC-OFDM
Carrier multiplexing in a channel bandwidth	Single analogue carrier per Channel	One or Multiple analogue carriers per Channel	One or Multiple analogue carriers per Channel
Examples	LTE uplink	DVB-S2, DVB-S2X	DVB-NGH

This evaluation is performed in similar configurations as existing standards.

5.2 DSNG use case

5.2.1 Introduction

The most straightforward way of transmitting modulated information consists in using single carrier sequential transmission of modulation signals as described in Figure 2. Bit interleaved coded modulation symbols (e.g. X-APSK symbols) are mapped into physical layer frames of specified formats. Base-Band Filtering and quadrature modulation shape the signal spectrum (for example squared-root raised cosine with different roll-off factors) before sending it in the RF satellite channel. In the present document this waveform will be denoted as SC-TDM.

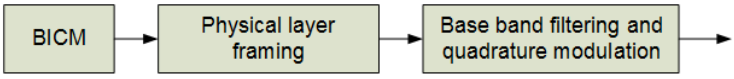

Figure 2: SC-TDM waveform generation

DVB-S2 [i.1] and DVB-S2X [i.2] use SC-TDM waveform. DVB-S2 employs QPSK, 8PSK, 16APSK and 32APSK with α = 0,35 or 0,25 or 0,20. DVB-S2X reuses the DVB-S2 physical layer and employs in addition higher modulation orders (64APSK, 128APSK and 256APSK) and sharper roll-off factors (α = 0,15 or 0,10 or 0,05) to improve the spectral efficiency.

SC-FDMA is a waveform that was introduced to improve the spectral efficiency in terrestrial networks. The goal of the present document is to show that it is suitable for satellite communications too.

SC-FDMA waveform has been adopted for the uplink air interface of 3GPP LTE [i.3], in commercial use since 2009. In a 3GPP LTE context, SC-FDMA represents not only the uplink waveform but also the multiple access scheme, the users sharing the uplink channel in the frequency domain by being allocated different groups of adjacent subcarriers like in a classic OFDMA system.

In the satellite world, SC-FDMA has been adopted as one of the waveforms for the satellite profile of DVB-NGH [i.4] under its full spectral allocation form SC-OFDM [i.5]. SC-FDMA was also acknowledged as a promising technique for future developments of DVB-RCS2 ([i.6], annex C). Moreover, the ITU-R recently issued its Recommendations [i.7] for the satellite component of the IMT-Advanced radio interface(s) where both validated air interfaces rely on SC-FDMA-based waveforms.

A SC-FDMA transmitter can be implemented in the frequency domain under the form of Discrete Fourier Transform (DFT) - precoded OFDM waveform as described in Figure 3.

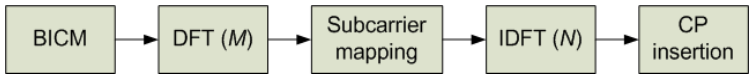

Figure 3: SC-FDMA waveform generation

Bit interleaved coded modulation symbols (e.g. X-APSK symbols) are grouped in blocks of M symbols and are precoded by an [MxM] DFT matrix. The M-sized output vector is then mapped onto M subcarriers represented by M out of N inputs of the inverse DFT. N_{guard} guard subcarriers are inserted at band edges on the remaining inputs. After an N-point Inverse Discrete Fourier Transform (IDFT), an N_{CP}-length CP may be inserted. In systems where the transmitted signal experiences a multipath frequency selective channel, the role of the CP is to absorb the channel delays and thus eliminate the interference between successive SC-FDMA symbols. In satellite scenarios, where the channel is essentially line of sight with practically no frequency selectivity, the insertion of a CP is not necessarily mandatory, depending on the FFT size, except when this CP is used to compensate time differences between the transmitters as is the case in RCS2use case. Roll-off can optionally be implemented in the frequency domain, after DFT precoding. SC-FDMA is compatible with zero roll-off implementations in a native manner.

In systems where there is no user specific multiple access (e.g. broadcasting on the forward link), or where multiple access is achieved by other means, SC-FDMA with full spectral allocation is called SC-OFDM in order to clarify the fact that SC-FDMA is only used as a waveform, and not as a multiple access scheme [i.22]. Since all data subcarriers are active, there is no null subcarrier insertion in the subcarrier mapping process and thus $N_{guard} = N\text{-}M$.

Time-domain implementations of SC-OFDM are also possible both at the transmitter and receiver sides. Nevertheless, less complex frequency domain implementations are usually preferred in practice.

5.2.2 Challenges

Thanks to a natural zero-roll off, SC-FDMA improves the spectral efficiency in linear communications channels. However, what does happen in a satellite non-linear channel? The sensibility to non-linear effects depends on the PAPR characteristics of the waveform.

During SC-FDMA waveform generation, DFT precoding restores the SC-like properties of the signal, alleviating the high PAPR problem specific to OFDMA signals. Localized and distributed subcarrier allocations have the same envelope variations as classical SC transmission [i.8]. Other types of allocation may degrade the PAPR. In the case of SC-OFDM, since all subcarriers are allocated, the PAPR is thus identical to that of a SC signal.

For SC-FDMA, roll-off can optionally be implemented in the frequency domain, after DFT precoding, at subcarrier level by the means of low complexity frequency domain processing. Nevertheless, SC-FDMA is by its nature compatible with zero roll-off. When employed, the roll-off controls both the excess bandwidth and the envelope variations of a signal. While high roll-off values reduce the signal's peak to average power ratio (PAPR), they also increase the excess bandwidth, which penalizes the system's performance due to either frequency mask filtering issues, or to increased inter-channel interference in multiple carriers per transponder scenarios.

SC-FDMA and SC transmission having the same roll-off factor display the same envelope variations, as further described in relation to Figure 4.

The CCDF of PAPR, as defined in equation below as CCDF of instantaneous amplitudes (sample level), indicates that at least one peak per block has an important amplitude and is susceptible to suffer clipping or severe distortion with a certain probability, but gives no information on how many samples in that block are distorted. Yet, all of these samples having important amplitudes cause degradation when passing through a nonlinear HPA. Severely clipping one single peak in a large block has a negligible effect, while distortion (even mild) of a large number of samples might have important consequences.

The distribution of the INP of a generic discrete signal v containing N_s symbols is defined as the probability that its instantaneous normalized power is above a certain threshold γ^2:

$$\mathrm{CCDF(INP)} = \Pr\left\{ \frac{\overbrace{|v[n]|^2}^{\mathrm{INP}(\mathbf{v})}}{\frac{1}{N_s}\sum_{k=0}^{N_s-1}|v[k]|^2} > \gamma^2 \right\}.$$

The CCDF of INP and the CCDF of PAPR tend asymptotically to the same value, but in the range of lower values of γ^2 the CCDF of INP has a better resolution.

Figure 4 presents the CCDF of INP of SC-TDM and SC-FDMA waveforms with QPSK mapping and with different roll-off factors. Signals are oversampled 4 times before CCDF computation. For SC-FDMA, N = 2 048, M = 1 728.

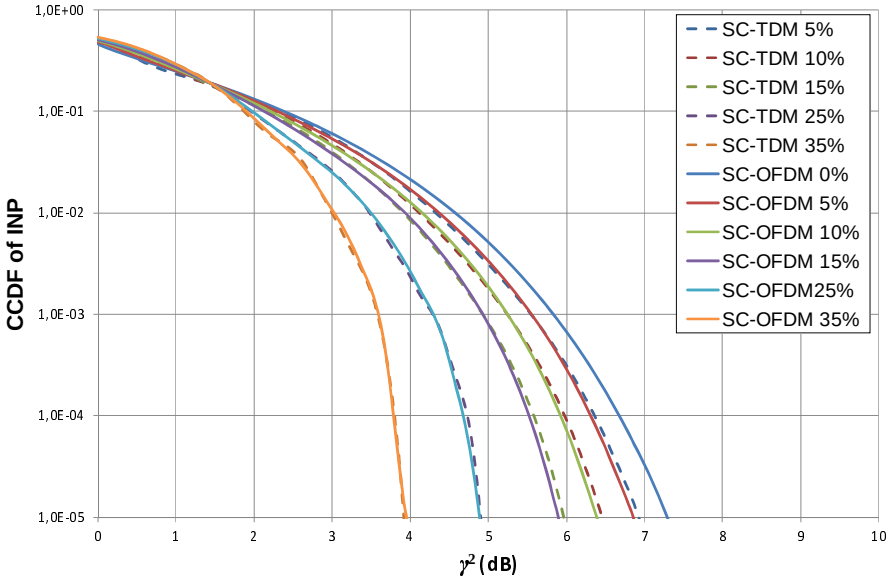

Figure 4: CCDF of INP for SC-TDM and SC-FDMA/SC-OFDM with different roll-off factors

5.2.3 Evaluation methodology

5.2.3.1 Introduction

To compare the performance of the two waveforms described here above, an evaluation framework is defined for the return link. This framework corresponds to the DSNG use case as defined in DVB-S2x [i.10]. Suitable channel models for performance evaluation of DVB-S2/S2X in the various application areas are given in [i.10] and [i.11].

5.2.3.2 System model description

5.2.3.2.1 General system model

Transmission over a transparent satellite transponder is depicted in Figure 5.

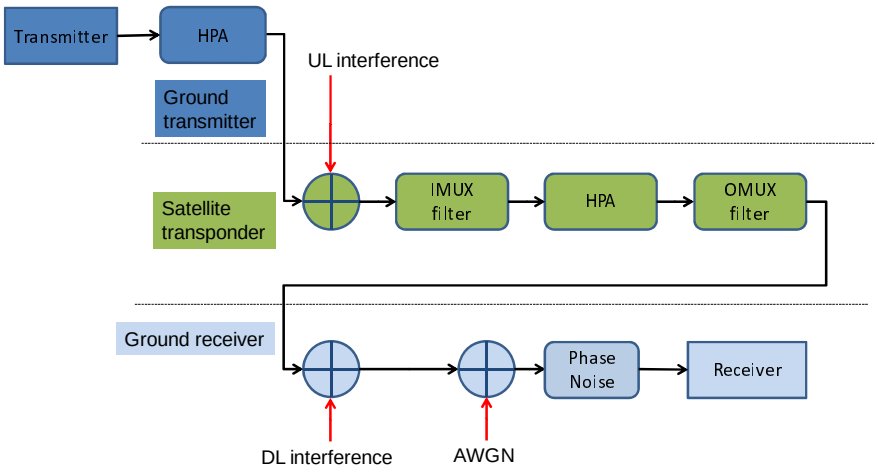

Figure 5: System model

5.2.3.2.2 Ground transmitter

A ground transmitter (terrestrial gateway, SNG van, etc.), generates signal representing the data to be transmitted, physical layer headers and possible pilot symbols. This signal modulated and framed either as described in Figure 2 to obtain a SC-TDM transmitted signal in conformity with the DVB-S2/S2X specifications [i.1] and [i.2], or as described in Figure 3 to obtain a SC-OFDM signal. The signal is then transmitted onto the current carrier to the satellite transponder. Uplink (UL) interference is modelled by adding in the adjacent channel a different signal carried by the same type of waveform as the current transmission. Ground transmitter HPA is considered either ideal or satisfying the characteristics in clause 4.4.1.1 of [i.11].

5.2.3.2.3 Satellite transponder

The transponder is composed of an input filter (IMUX) selecting the current carrier, a high power amplifier (HPA) representing the non-linearity on board of the satellite and an output filter (OMUX) who reduces the out-of-band emission due to the spectral regrowth after the HPA. IMUX and OMUX amplitude and group delay response models are drawn from annex H.7 of the DVB-S2 specifications [i.1] and scaled for a reference transceiver bandwidth of 38 MHz. They are given in Figure 6. HPA is considered either ideal (linear channel) or non-linear TWTA. Two non-linear TWTAs are considered, the conventional and the linearized TWT as drawn from [i.11] with AM/AM and AM/PM characteristics given in Figure 7.

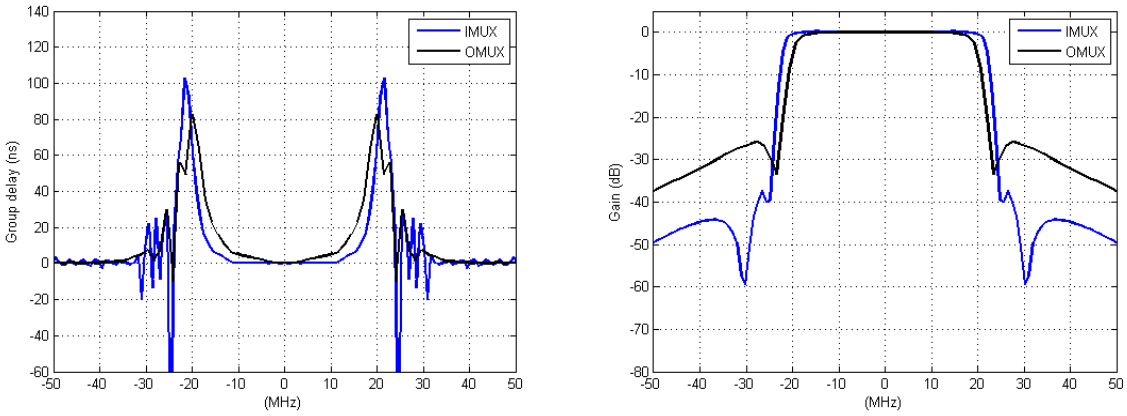

Figure 6: IMUX and OMUX filter characteristics

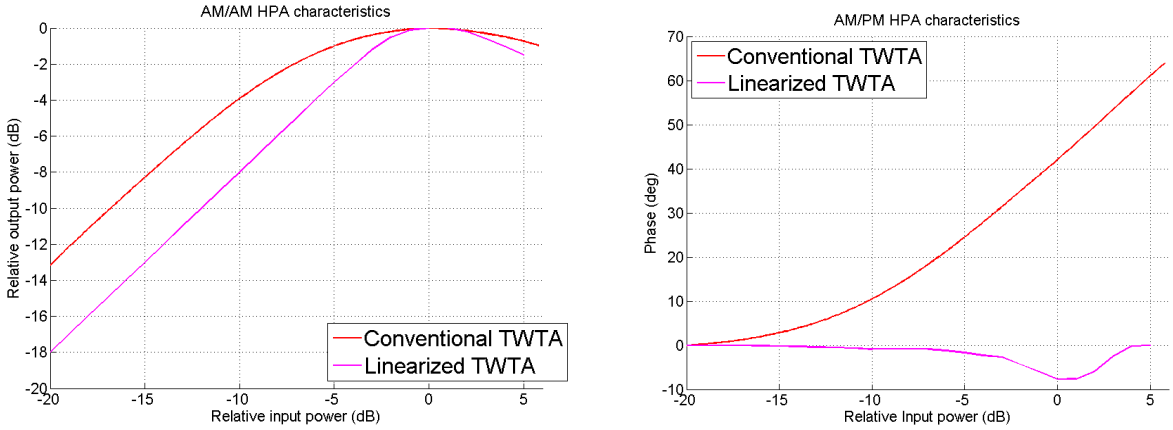

Figure 7: Conventional and Linearized TWTA characteristics

5.2.3.2.4 Ground receiver

At the ground receiver, the useful signal is corrupted by adjacent downlink (DL) interferers, AWGN and optional phase noise. When the presence of phase noise (PN) is simulated, the critical mask drawn in Figure 8 and described in annex H.8, table H.4 of the DVB-S2X [i.2] is used.

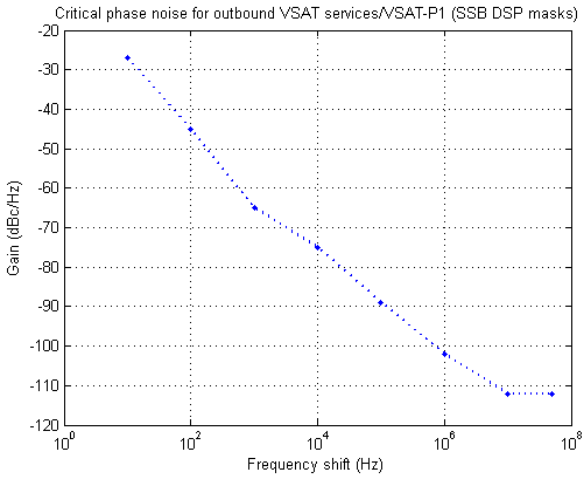

Figure 8: Phase noise characteristics

The receiver is either a classical time-domain SC-TDM receiver with fractional equalization or a SC-OFDM receiver with frequency domain per subcarrier equalization. Equalization is followed by a time-domain linear phase noise correction.

Ideal frequency synchronization is considered. Time synchronization is genie-aided (based on correlation with the transmitted signal, ideally supposed as known). Linear minimum mean square error (MMSE) equalization is employed using long-term auto-correlation and cross-correlation coefficients computed through a genie-aided approach. Phase noise estimation and correction is realistic, based only on Start of Frame sequence and pilot resources of S2 frame. A simple method reduced to a piecewise linear interpolation between reference resources is used [i.11]. For both waveforms, phase noise compensation is performed after equalization, at symbol rate.

The SC-TDM receiver, depicted in Figure 9, employs a fractional time domain equalization implemented in the time domain with a N_{taps} = 41 taps finite impulse response filter with an oversampling rate *ovs* = 2.

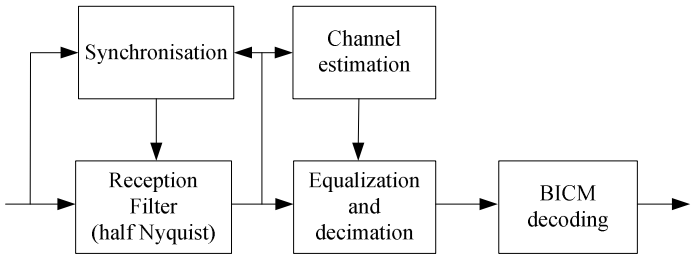

Figure 9: SC-TDM receiver

SC-FDMA receiver, depicted in Figure 10, performs low-complexity equalization in the frequency-domain, allowing an important reduction of the number of required operations with respect to time-domain equalization. Frequency domain equalization is performed at subcarrier level (one coefficient per subcarrier), after DFT.

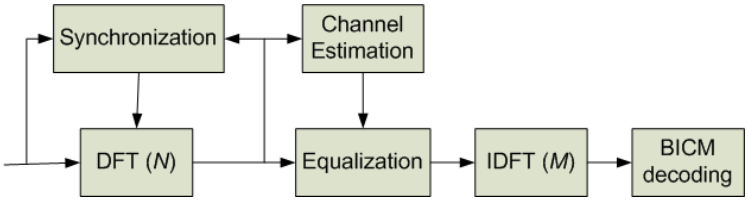

Figure 10: SC-FDMA/SC-OFDM receiver

5.2.3.3 DSNG simulation scenario

A professional use case scenario of video contribution and distribution is considered. One or several video contributors share the same transponder, making either simple or multiple carrier usage. The cases of one, two and four contributors are represented in Figure 11 a), b) and c) respectively. In case of several-carrier usage, each carrier is used by a different operator, which optimizes his scheme independently and uses its own IMUX/OMUX pair.

Carrier spacing is denoted Δf as in Figure 11 d).

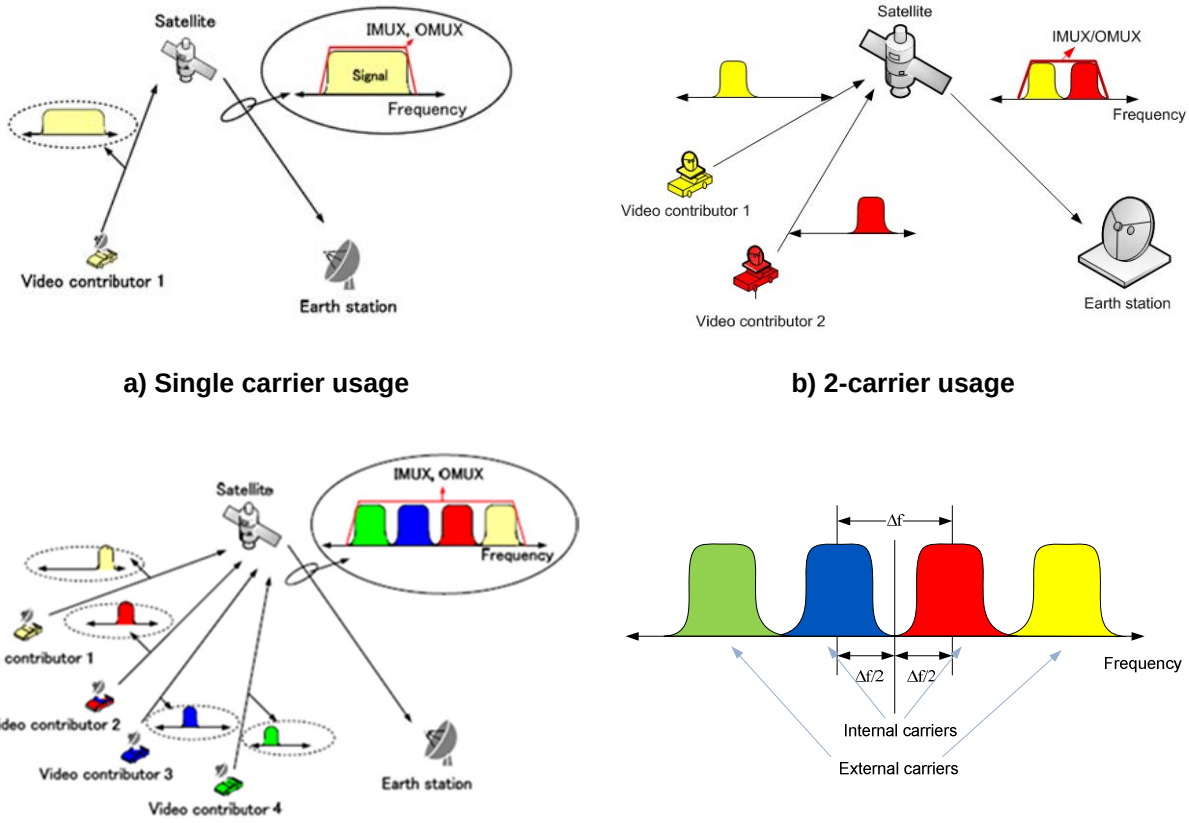

a) Single carrier usage **b) 2-carrier usage**

c) 4-carrier usage **d) Carrier spacing for multiple carrier usage**

Figure 11: Video contribution and distribution use case

In a single carrier scenario, the multiple access is performed in TDMA or by using different transponders. Note that this can be performed also in the multiple-carrier scenario.

5.2.3.4 Simulation methodology

Performance is evaluated as following, in compliance with [i.10] and [i.11].

In a first step, in non-linear channels, for each MODCOD the optimum functioning point of the HPA is determined. The input/output back-off (IBO/OBO) is defined as the measured power ratio (in dB) between the input/output signal power and the HPA's saturation level. A large range of IBO values was tested and for each such value the MODCOD's performance is represented under the form of Packer Error Rate (PER) versus CSat/*N*, where CSat is the signal power at the output of the IMUX and *N* is the AWGN level at the input of the receiver measured in the reference bandwidth of 38 MHz divided by the number of carriers N_{car} per transponder. CSat/*N* is thus representative of the signal-to-noise ratio (SNR) at the input of the receiver, plus a penalty caused by OBO and OMUX filtering. The HPA optimum functioning point (corresponding to a couple (IBO_{opt}, OBO_{opt})) was selected as the one maximizing the performance for a target PER = 10^{-3}. Here, maximizing the performance means minimizing CSat/N. All following simulations for each MODCOD are considered as being performed at its optimal IBO_{opt}. In addition to the required CSat/*N*, the corresponding spectral efficiency (SE) was considered, for the reference bandwidth of 38 MHz/(as bandwidth reference is constant, this metrics is proportional to the total data rate per transponder). Strictly speaking, this spectral efficiency is calculated as $SE = \rho \times N_{bits} \times R_s / (38.10^6 / N_{car})$ (b/s/Hz), where ρ is the code rate.

In a second step, modulation rate (R_s) (for all use cases) and carrier spacing Δf (for multiple carrier usage use cases) are optimized. This optimization is conducted separately for SC-TDM and SC-FDMA/SC-OFDM. For all MODCODs (at their respective IBO_{opt}) a range of different (Rs, Δf) values was tested and PER versus CSat/N performance was plotted. The CSat/*N* values were identified for a target PER=10^{-3} and the associated spectral efficiency and for each tested (Rs, Δf) couple, the variation of spectral efficiency (given by the different MODCODS) was plotted versus CSat/*N*. The optimum $(Rs, \Delta f)_{opt}$ couple was selected as the one overall maximizing the performance (i.e. minimizing CSat/N and maximizing the spectral efficiency). For multiple carrier usage, simulation results show that, for all scenarios, the optimum carrier spacing Δf_{opt} equals the reference transponder spacing divided the number of used carriers, i.e. Δf_{opt} = 20 MHz for 2-carrier usage and Δf_{opt} = 10 MHz for 4-carrier usage.

5.2.4 Performance analysis

5.2.4.1 Spectral efficiency

5.2.4.1.1 Introduction

In the performance figures, the spectral efficiency SE is drawn versus CSat/N. The gain (or no gain) depends on CSat/N. In order to synthesize the results, three SE range values were considered:

- Small data-rate: 1,6 - 2 b/s/Hz
- Medium data-rate: 2 - 3,5 b/s/Hz
- High data-rate: 3,5 - 6 b/s/Hz

For each SE range, the average SE was calculated for each transmission mode, which allows to simply compare the waveforms in Table 3, Table 4 and Table 5.

5.2.4.1.2 Single carrier usage

The results for the single carrier usage are depicted below. The results are provided without any HPA ("No HPA"), or with the linearized HPA ("Lin. HPA") or with the Conventional HPA ("Conv. HPA"). They are also provided with phase noise ("PN") or without phase noise (no "PN" mention).

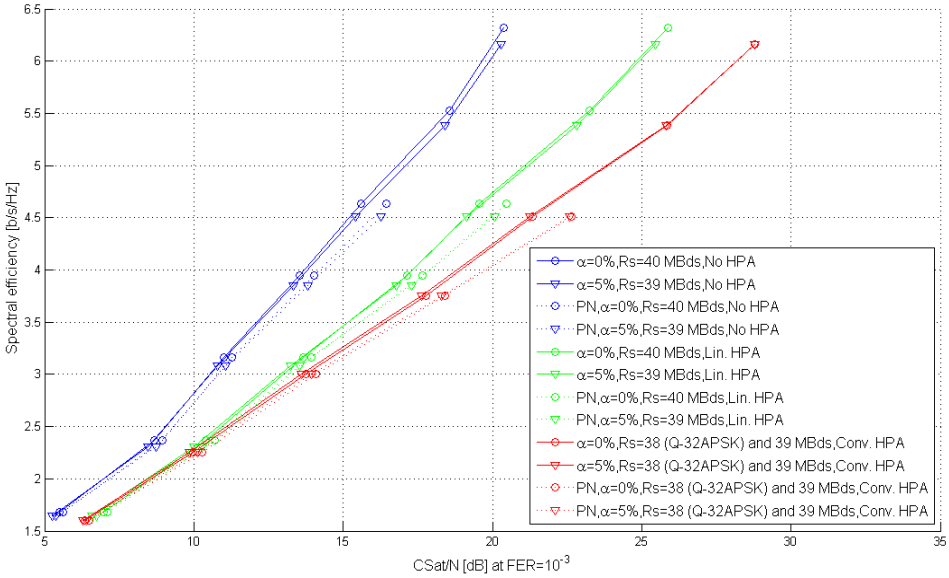

Figure 12: Single carrier usage performance

α = roll-off.

Table 3 compares performances of SC-FDMA/SC-OFDM with zero roll-off to SC-TDM with 5 % roll-off. This comparison is performed for each SE range and for each amplifier, with and without PN.

Table 3: SE gains of no roll-off over 5 % roll-off, single carrier usage

	Low SE (0,45 - 2 b/s/Hz)		Medium SE (2 - 3,5 b/s/Hz)		High SE (3,5 - 6 b/s/Hz)	
	No PN [%]	PN [%]	No PN [%]	PN [%]	No PN [%]	PN [%]
No HPA	0,5	0,7	0,1	0,4	1,2	1,1
Linearized HPA	-0,9	-0,8	-0,9	-0,8	0,2	0,3
Conventional HPA	-0,9	-1	-1	-0,9	-0,4	-0,5

In this scenario, with an HPA, the zero roll-off system (SC-FDMA) only brings a small advantage for large spectral efficiencies, above 3,5 b/s/Hz. Taking into account the phase or not does not change the conclusions. As expected, with no HPA, the zero roll-off system always improves performances.

5.2.4.1.3 Double carrier usage

The following figures provide the same results in the two-carrier use case. The different parameters, e.g. Rs or Δf, were optimized for each specific scenario.

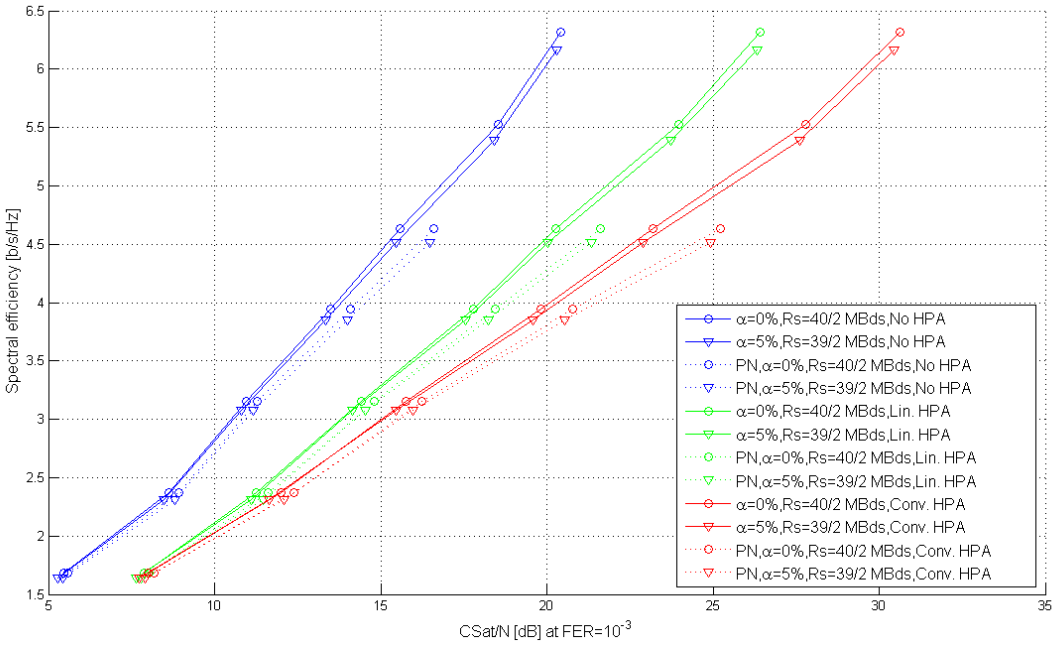

Figure 13: Double carrier usage performance

Table 4: SE gains of no roll-offs over 5 % roll-off, double carrier usage

	Small SE (0,45 - 2 b/s/Hz)		Medium SE (2 - 3,5 b/s/Hz)		High SE (3,5 - 6 b/s/Hz)	
	No PN [%]	PN [%]	No PN [%]	PN [%]	No PN [%]	PN [%]
No HPA	1,1	1,3	0,9	1,2	1,5	1,8
Linearized HPA	0,6	0,9	0,6	0,8	1,1	1,3
Conventional HPA	0,4	0,6	0,2	0,5	1,4	1,4

In this scenario, with a linearized HPA, the zero roll-off system (SC-FDMA) brings an advantage for large spectral efficiencies, above 3,5 b/s/Hz. Taking into account the phase or not does not change the conclusions. As expected, with no HPA, the zero roll-off system always improves performances. However, in this case, with a conventional HPA, the 5 % roll-off systems remains always better.

5.2.4.1.4 Four and more carrier usage

Figures 14 and 15 provide the same results in the four-carrier use case. The different parameters, e.g. Rs or Δf, were optimized for each specific scenario. For this four carrier usage, performances are provided for the inner carriers and the outer carriers.

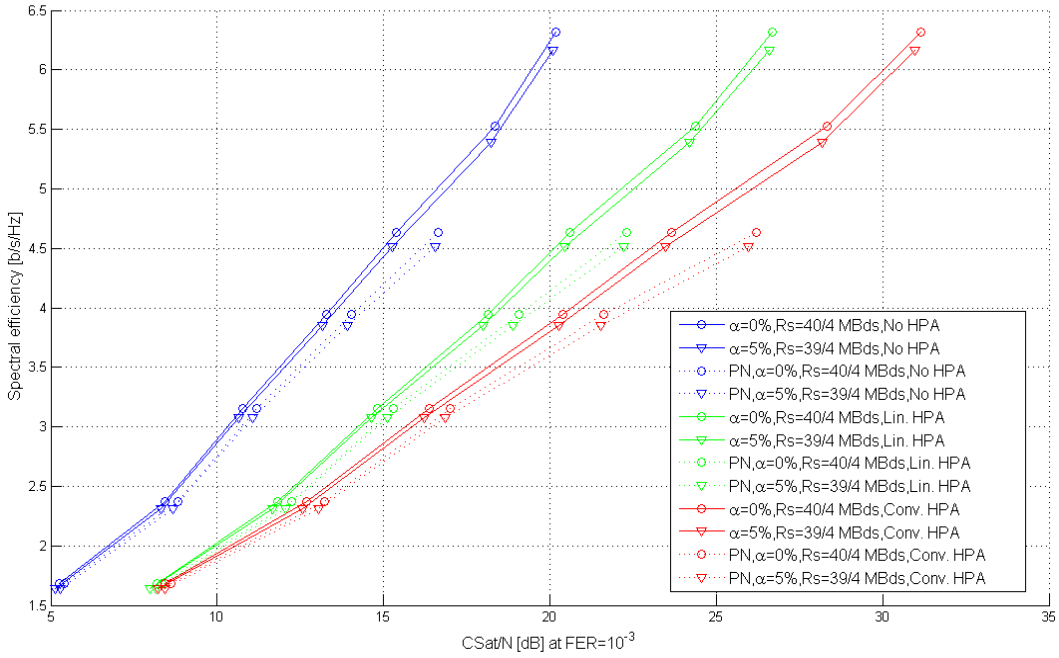

Figure 14: Four carrier usage performance, inner carriers

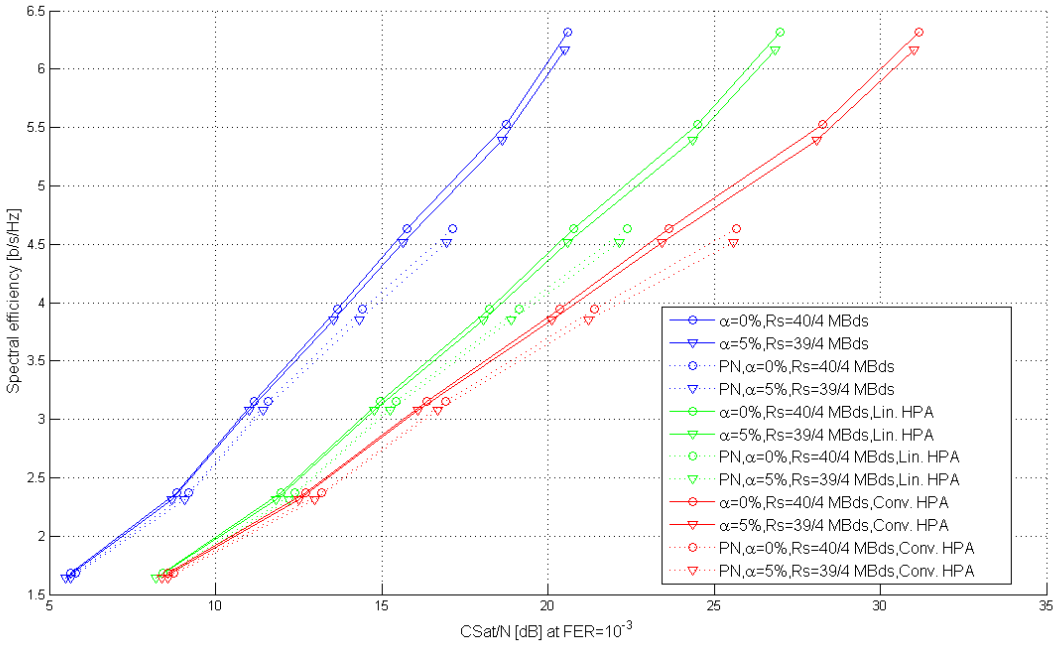

Figure 15: Four carrier usage performance, outer carriers

Table 5: SE gains of null roll-offs over 5% roll-off, four carrier usage

		Small SE (0,45 - 2 b/s/Hz)		Medium SE (2 - 3,5 b/s/Hz)		High SE (3,5 - 6 b/s/Hz)	
		No PN [%]	PN [%]	No PN [%]	PN [%]	No PN [%]	PN [%]
Outer carriers	**No HPA**	1,2	1,4	1,1	1,2	1,7	1,7
	Linearized HPA	1,1	1,2	1	1	1,5	1,4
	Conventional HPA	1,2	1,4	0,8	1,1	1,5	1,8
Inner carriers	**No HPA**	1,4	1,5	1,2	1,3	1,7	1,8
	Linearized HPA	1,1	1,2	1,1	1,1	1,6	1,6
	Conventional HPA	1,2	1,4	1,4	1,4	1,7	2

In this scenario, for all amplifiers, the zero roll-off system (SC-FDMA) brings an advantage over the 5% roll-off systems. With four carriers, the PAPR is degraded in all cases and the amplifiers are working in a linear region; therefore the PAPR penalty of a zero roll-off system becomes negligible.

5.2.4.2 Complexity

In this clause, the complexity of a SC-FDMA scheme with a frequency domain implementation was compared to the complexity of a SC-TDM scheme, 5 % roll-off, with a classical time domain implantation. For this complexity comparison between frequency domain and time domain only the different parts were considered, i.e. waveform generation (transmission, FDT and TDT) and reception equalization (FDE and TDE). In the following table, a 'cell' should be understood according to DVB terminology. In this context, it corresponds to a transmitted constellation symbol.

Table 6: Time domain and frequency domain complexity comparison

	Variables definition	Number of multiplication per cell	Examples
FDT	*M, N* : DFT and IDFT sizes	$(M/2\log_2(M) + N/2\log_2(N) + M\times\alpha)/M$	$\alpha = 0$; $N/M = 1,2$ $M = 6\,912 \Rightarrow 14,1$ $M = 27\,648 \Rightarrow 16,3$
TDT	Ovs : oversampling ratio L_{FIR} FIR duration in T_s	$N_{taps} = Ovs * L_{FIR}+1$	$\alpha = 5$ % $Ovs = 2$ $L_{FIR} = 60$ $N_{taps} = 120$
FDE	*M, N* : DFT and IDFT sizes α : Roll-off	$(M/2\times\log_2(M) + N/2\times\log_2(N) + M\times(1+\alpha))/M$	$\alpha = 0$; $N/M = 1,2$ $M = 6\,912 \Rightarrow 15,1$ $M = 27\,648 \Rightarrow 17,3$
TDE	*Ovs* : oversampling ratio L_{FIR} FIR duration in T_s	$N_{taps} = Ovs * L_{FIR} + 1$	$\alpha = 5$ % $Ovs = 2$ $L_{FIR} = 20$ $N_{taps} = 41$

For the considered functions, a frequency domain implementation allows to decrease the complexity. With the considered hypothesis, the number of multiplications is divided by about 6 at the transmitter, and by a ratio between 2 and 3 at the receiver.

5.2.5 Synthesis

With an HPA and one carrier usage, radio interfaces with 5 % roll-off (SC-TDM or SC-FDMA) offer better performances than a 0 % roll-off radio interface (SC-FDMA). However, for multi-carrier usage, SC-FDMA with 0 % roll-off outperforms SC-TDM with 5 % roll-off in terms of spectral efficiency. In this case, the gain in spectral efficiency offered by 0 % roll-off is between 1 % and 2 %.

Moreover, a frequency domain implementation allows decreasing the complexity of both the transmitter and the receiver. This frequency domain implementation is eased with the SC-FMDA waveform.

Performance comparison is provided in Table 7 at high spectral efficiencies, for the different DSNG scenarios and a linearized amplifier, together with a complexity comparison.

Table 7: Synthesis of SC-FDMA and SC-TDM comparison (for 0 % and 5 % roll-off respectively, and a linearized amplifier)

DSNG		SC-FDMA and SC-TDM comparison at high spectral efficiency
Spectral Efficiency	Single carrier usage	0/2/0,3 % SC-FDMA gain
	Two carrier usage	1,1/1,3 % SC-FDMA gain
	Four carrier usage	1,1/1,6 % SC-FDMA gain
Complexity		Number of multiplications in the equalizer divided by 2-3 for SC-FDMA

5.3 Broadband access use case

5.3.1 Introduction

The state-of-the-art standards for satellite communications in a broadband access (DVB-RCS2) return link utilize a Time Division Multiple Access (TDMA) waveform in the air interface. Single-Carrier Frequency Division Multiple Access (SC-FDMA) has been considered as an option in the DVB-RCS2 standard. This is thanks to its confined spectrum of orthogonal subcarriers, low-complexity frequency domain equalization and moderate Peak-to-Average Power Ratio (PAPR). However, power efficiency optimization and measures to minimize the impact of the nonlinearities of the satellite channel are still an open issue. The inherently confined spectrum of SC-FDMA enables the reduction of the guard bands between physical carriers. However, the orthogonal subcarriers require accurate time and carrier frequency synchronization, especially on the user uplink. For a successful synchronization acquisition, the frame timing offsets of the users need to be estimated at log-on. This is generally achieved via the random access channel, where the procedure needs to be tailored to the delay constraints of the satellite link. For a successful synchronization tracking, fine synchronization algorithms are required to correct the residual timing and frequency errors. Due to the more stringent synchronization requirements of the waveforms, improved algorithms for synchronization acquisition, tracking, estimation and compensation need to be designed and analysed.

In the present document, SC-FDMA is studied in comparison with TDMA, as well as Orthogonal Frequency Division Multiple Access (OFDMA), for application in the DVB-RCS2 satellite return link. Practical synchronization algorithms have been evaluated and suitable solutions for synchronization acquisition and tracking have been proposed. For synchronization acquisition, the framework from terrestrial LTE system is adapted to transmission over satellite. In particular, the timing alignment algorithm and the preamble design of the LTE random access channel are adapted to accommodate for large satellite propagation delays. A GPS-based approach for delay pre-compensation has been proposed for synchronization acquisition. It is able to increase the synchronization accuracy from the milliseconds range to the nanoseconds range. In addition, the Mengali and Morelli algorithm for timing offset estimation and the Moose algorithm for frequency offset estimation have been tested as a part of a SC-FDMA receiver simulation, and they show considerable improvement of the synchronization accuracy. In addition, the power and spectral efficiencies of the waveforms have been optimized by means of a novel receiver implemented at the gateway. First, the total degradation (TD) in the OFDMA, SC-FDMA and TDMA waveforms is minimized as a function of the output power back-off. The improvements of the power and spectral efficiencies are then compared. SC-FDMA shows an overall better spectral efficiency and an improvement of around 1 dB in power efficiency as compared to state-of-the-art TDMA in the return link. Finally, the computational complexity of the waveforms has been evaluated.

5.3.2 Challenges

5.3.2.1 Synchronization over the satellite channel

In SC-FDMA, as well as in OFDMA, the analogue carrier is further subdivided in digital subcarriers, whereby a portion of the subcarriers are dedicated to a user. The spectrum division is illustrated in Figure 16. The main difference with the previous use case is that here only a portion of the digital subcarriers is allocated to a user. The multiple access is performed in a SC-FDMA/OFDMA fashion. At a user terminal, only the subcarriers of the one user are modulated, and the rest are set to zero. The user signals superimpose over the satellite channel, and they are collectively decoded at the gateway. As a result there are tight synchronization requirements.

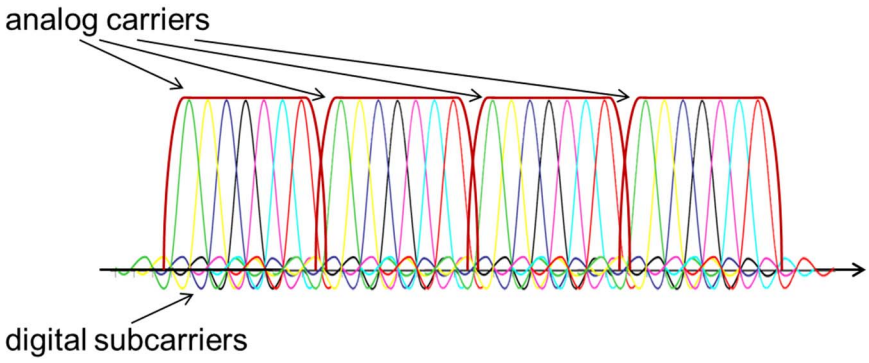

Figure 16: Spectrum division in SC-FDMA and OFDMA in the return link

SC-FDMA is a multicarrier air-interface, which makes use of orthogonal subcarriers. Orthogonality requires timing precision in both uplink and downlink transmissions. In particular in the uplink, different users with different propagation delays transmit to the Network Control Centre (NCC) on different subcarriers within the same uplink frame. In order to maintain orthogonality, it is essential that all UEs (User Equipment) are time synchronized at the NCC. Synchronization in SC-FDMA is a topic investigated often in literature [i.12], and some approaches have been implemented for the LTE air interface [i.13]. The waveforms depend strongly on frame timing and carrier frequency synchronization of all users in order to mitigate Inter-Symbol Interference (ISI), inter-carrier interference (ICI) and Multiple Access Interference (MAI).

For what concerns synchronization acquisition the focus is on frame timing offsets estimation at log-on in order to correct differential propagation delays in the presence of residual frequency offsets and amplifier non-linearity. This is achieved via Random Access (RA) for the SC-FDMA uplink in LTE but it may be different for the satellite implementation. Timing alignment of the uplink transmissions is achieved by applying a timing advance at each user, relative to the received downlink timing [i.13], to accommodate the differential propagation delays within the length of the cyclic prefix (CP). The Physical Random Access Channel (PRACH) in LTE is dimensioned with a Guard Time (GT) to accommodate the Round Trip Time (RTT). The PRACH preamble is an SC-FDMA symbol derived from Zadoff-Chu (ZC) sequences due to their constant amplitude zero autocorrelation (CAZAC) properties, [i.14] and [i.15]. The requirements of SC-FDMA synchronization acquisition over a GEO satellite link are similar to those of LTE in terms of accuracy. However, the challenges are greater, mainly due to the larger propagation delays in the satellite channel with RTT of 500 ms as compared to the order of μs in the terrestrial link. Furthermore, the maximum differential propagation delay within a GEO spot beam is of the order of ms. Given a typical SC-FDMA symbol duration of the order of μs, a guard time greater than the satellite RTT or maximum differential propagation delay is not affordable within an integrated PRACH. One approach to solve this problem is to use a dedicated PRACH for the satellite channel but the loss in spectral efficiency due to the overhead is not desirable. An alternative solution is proposed to enable the use of integrated PRACH.

For what concerns tracking, it is assumed that after log-on the magnitude of residual symbol timing and carrier frequency errors fall within defined limits, as CP length for timing errors, and half of the carrier spacing, for frequency errors. Residual errors can be further reduced with fine synchronization algorithms provided that terminals periodically transmit pilot symbols interleaved with traffic and that each user exploits a subset of adjacent subcarriers. In general, timing and carrier frequency errors result in a static easily predictable offset with superimposed short-term variations, i.e. attenuation and phase rotation of the useful signal component plus ICI. In a multi-carrier access network it is convenient to eliminate the static timing and carrier offsets by correcting the local references of terminals [i.12]. Short-term parameter variations, less tolerant to the satellite feedback delay, are to be corrected directly at the gateway using a closed loop. In general, synchronization step over satellite has to cope with symbol timing inaccuracies provoked by a set of physical causes [i.16] such as the mismatch between transmitter and receivers clock synchronization, local oscillator drift, due to a clock frequency offset or to short-term instability, satellite drift around the GEO orbit that introduces a frequency drift (Doppler effect), and variations in the path length due to ionosphere or troposphere effects.

To derive practical estimators for timing errors it can be noted that the problem under analysis is similar to the estimation of the angular frequency of a discrete-time complex sinusoid embedded in additive noise. After a literature review of the subject, different algorithms have been identified (Rife and Boorstyn, Kay, Luise and Reggiannini, Mengali and Morelli) and investigated. It has been highlighted how Mengali and Morelli [i.17] algorithm outperforms the other algorithms attaining the Cramér-Rao bound with fixed estimation range down to very low SNRs and gives the best compromise between performance, complexity and range. On the other side, a simple way to estimate the carrier frequency offset has been proposed by Moose [i.18]. The algorithm is based on comparing phase shifts between the FFT samples in a couple of identical pilot symbols transmitted in different symbol intervals. In particular, Moose suggests to sum the cross products between FFT samples with the same index and take the argument of the result. It can be proven that this is the Maximum Likelihood Estimator (MLE) of the parameter under investigation.

5.3.2.2 Minimization of non-linear distortion in the satellite channel

In a DVB-RCS2 return link use case, a number of carriers are allocated to the users in a beam. The satellite transponder is in multi-carrier mode, and as a result the common assumption is made that the intermodulation interference (IMI) at the satellite is transformed into Gaussian noise, reducing the thermal link budget. Since the analogue carriers are much narrower than the spectral response of the IMUX and OMUX filters on board the satellite, a flat fading frequency non-selective channel is considered. In addition, since a single gateway receives the signals of the user terminals in the entire beam, no phase noise is considered at the receiver. Therefore, the focus of the power and spectral efficiency optimization in this study is on minimization of the IMI caused by the amplifier at the user terminal. Since this amplifier is driven in single-carrier mode in state-of-the art Time Division Multiple Access (TDMA) employed in DVB-RCS2, the IMI is correlated with the signal, resulting in the well-known constellation warping effect. As a result, optimization of the OBO is required, in order to maximize the error-rate performance, e.g. minimization of the bit-error rate (BER).

5.3.3 Evaluation methodology

5.3.3.1 Synchronization acquisition

The RTT in a GEO satellite link is significantly larger than what is obtainable in terrestrial cells (order of microseconds). However, the maximum differential propagation delay in GEO satellite spot beam (i.e. centre to edge of beam) is significantly lower than the RTT of 500ms but is still of the order of a few milliseconds as shown in Table 8. Given that a typical SC-FDMA symbol duration is of the order of microseconds as shown in Table 9, a guard time equal to the maximum differential propagation delay in a satellite beam (order of milliseconds) is not spectrally efficient and would require a dedicated RACH.

In order to support an integrated RACH (with efficient dimensioning for an SC-FDMA waveform) in the GEO satellite channel, the use of global-positioning-system-(GPS)-based delay pre-compensation is proposed for uplink timing alignment. The proposed uplink timing acquisition stages are shown in Figure 17. GPS-based timing pre-compensation requires the implementation of a GPS device at each return channel satellite terminal (RCST), which is considered affordable. The advantage of using this approach is that the RACH can be dimensioned with highly reduced overhead. This is because a GPS device located at each RCST will track its current location with substantial accuracy within approximately 10 m [i.19]. This can then be combined with the satellite location data and the NCC co-ordinates to calculate the specific propagation delay between the NCC and each RCST. The calculated relative delay can then be pre-compensated for each RCST before the random access procedure. The effect of using the proposed approach is that the timing misalignment between RCSTs is significantly reduced from the order of milliseconds to an order of nanoseconds as shown in Table 8. Using the proposed GPS-based delay pre-compensation technique, the guard time required for the RACH is reduced from about 5 ms to about 100 ns (a ratio of 50 000:1). A residual timing error of less than 100 ns necessitates CP dimensioning. This translates to a negligible overhead of less than 1 % and a power loss of 0,04 dB for SC-FDMA symbol with duration of 10 μs.

Table 8: Pre-compensation accuracy

Beam Radius (A)	600 km	300 km	100 km
Speed of light (C)	3×10^8 m/s	3×10^8 m/s	3×10^8 m/s
Approximate max. 2-way differential delay (D=2A/C)	4 ms	2 ms	0,67 ms
Min. position accuracy of GPS device (E)	10 m	10 m	10 m
Pre-compensation accuracy (F=2E/C)	67 ns	67 ns	67 ns

Table 9: SC-FDMA symbol duration

Carrier Bandwidth (A)	100 MHz	150 MHz	250 MHz
Subcarrier spacing, N_1 = 1 024, (B=A/N_1)	97,7 kHz	146,5 kHz	244,1 kHz
Symbol duration, N_1 = 1 024, (D=1/B)	10,2 us	6,8 us	4,1 us
Subcarrier spacing, N_2 = 4 096, (E=A/N_2)	24,4 kHz	36,6 kHz	61 kHz
Symbol duration, N_2 = 4 096, (F=1/D)	40,8 µs	27,2 µs	16,4 µs

Figure 17: Uplink Timing Acquisition Stages

For SC-FDMA synchronization acquisition, a conventional approach such as in LTE is to dimension the random access channel within an SC-FDMA superframe as shown in Figure 18. The RACH is dimensioned with appropriate guard times and guard tones to provide for isolation and tolerance to expected timing and frequency errors in the uplink. The random access preambles used in LTE are ZC sequences [i.13]. ZC sequences, also referred to as CAZAC sequences, are polyphase codes which have good periodic correlation properties and robust performance in the presence of frequency offset [i.14] and [i.15]. The constant amplitude property of ZC sequences makes them an attractive option for non-linear transmissions in the satellite return link. Some detection algorithms for ZC sequences in LTE are discussed in [i.20] and [i.21]. Using the conceptual SC-FDMA framing as shown in Figure 18, synchronization acquisition in the satellite return link can be achieved as follows. After downlink synchronization has been achieved, the parameters of the RACH established and GPS-based timing pre-compensation has been performed, each RCST transmits a random access preamble to the NCC. This is detected by the NCC and the appropriate timing error established as integer multiples of the OFDM sampling duration. The NCC then sends a timing advancement command to the RCST in order to pre-compensate for the detected timing errors. Each RCST acquire synchronization at logon in order to maintain a synchronous SC-FDMA system.

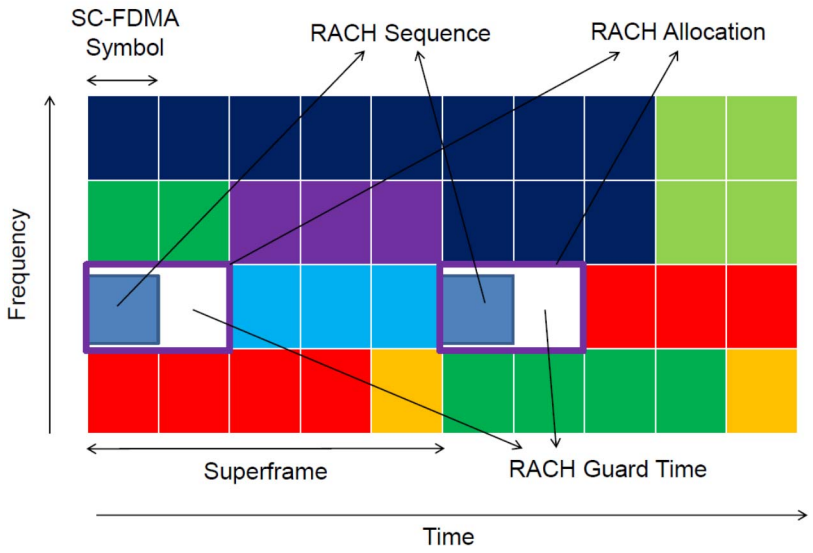

Figure 18: Conceptual SC-FDMA framing

5.3.3.2 Synchronization tracking

In order to assess the impact of synchronization tracking techniques on SC-FDMA return link, the assumed reference system model for the generic user *i* is composed of a SC-FDMA transmission/reception chain where an M-point Discrete Fourier Transform (DFT) is calculated to get the frequency domain representation of the M parallel symbols. Such set of M points is mapped over a set of N subcarriers assigned by the satellite gateway to the *i*-th user on the given uplink resource block. An N-point inverse DFT (IDFT) then modulates the signal and a CP is inserted before transmission over the air. On reception, the scheme is reversed and the gateway on its turn extracts (de-maps) the carriers associated to every user computing the IDFTs to reconstruct the user symbols.

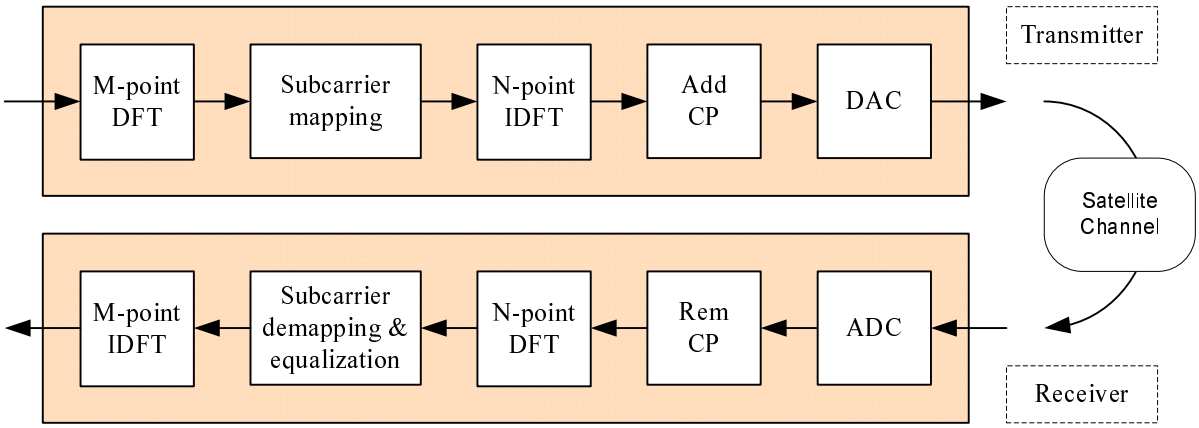

Figure 19: SC-FDMA for *i*-th user satellite uplink

On the basis of the analysis above, the techniques selected to be implemented in the system are:

- Moose algorithm, for residual carrier frequency offset (CFO) estimation purposes [i.18].
- Mengali and Morelli algorithm, for residual timing errors (TE) estimation purposes [i.17].

The core algorithms are implemented at the gateway side, after performing a coarse frame acquisition that reduces residual timing and frequency errors. In the simulation, the following set up has been identified.

Table 10: SC FDMA simulation setup

System FFT size	128 carriers
User FFT size	16 (sub)carriers
Cyclic prefix size	1/8th system FFT size (16 samples)
User pilot period	10 SC-FDMA symbols

5.3.3.3 Optimization of total degradation

In this study, a total of 2 048 subcarriers per analogue carrier are allocated to 32 users with 64 subcarriers per user. A single-carrier scenario is evaluated. In TDMA, pulse shaping is performed by means of an SRRCF with 20 % roll-off factor, as well as a tighter roll-off factor of 5%. These roll-off factors penalize the spectral efficiency respectively, which is in accordance with the 1+roll-off rule for inter-carrier spacing. In SC-FDMA and OFDMA, a guard band of 5 % is considered at the border between analogue carriers, in order to reduce the inter-carrier interference. In all the schemes, the performance of static data pre-distortion at the transmitter [i.11], a technique borrowed from the forward link, is compared with single-tap equalization at the receiver as means to compensate the channel. The AM/AM and AM/PM characteristics of a Solid State Power Amplifier (SSPA) in Ka band presented in Figure 20 are considered in this study. The user terminal in the return link employs QPSK, 8-PSK and 16-QAM constellations according to DVB-RCS2.

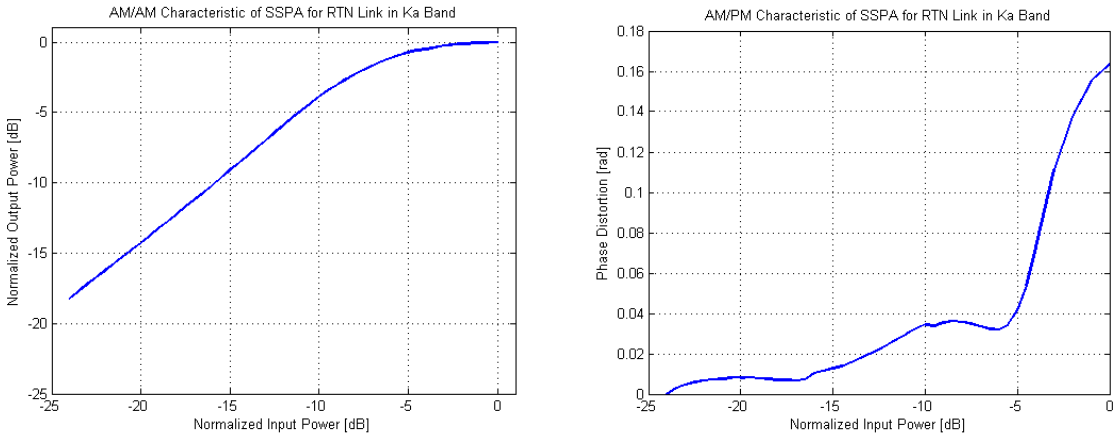

Figure 20: Normalized non-linear transfer characteristic of an SSPA in Ka band for the return link: AM/AM characteristic (left), AM/PM characteristic (right)

In order to quantify effective penalty on the electrical power induced by IMI of the amplifier nonlinearity, the total Degradation (TD) metric is defined as follows:

$$TD\ [dB] = OBO + SNR_{req.non\text{-}lin.chan.} - SNR_{req.lin.chan.}$$

In addition to the required OBO for a given maximum transmitted power level, the TD incorporates the penalty on the electrical SNR in order to achieve a target BER in the presence of the amplifier nonlinearity. This is expressed as the difference between the SNR requirement in the non-linear channel and the SNR requirement in the corresponding linear channel.

5.3.4 Performance analysis

5.3.4.1 Synchronization accuracy

In this clause, the performance of the synchronization tracking algorithms in the presence of CFO [i.18] and TE [i.17] is evaluated. In Figures 21 to 23, NC stands for *Not Compensated*, while C for *Compensated*. Figure 21 shows the performance in terms of mean squared error (MSE) of received constellation symbols at the input of the demodulator according to different values of normalized CFO and SNR. The MSE can be regarded as the inverse of the signal-to-interference (SIR) after the synchronization stage. A normalized CFO of 0,1 means that terminal and gateway oscillators are misaligned of $0{,}1 * \Delta f$, where Δf is the inter sub-carrier frequency space. In Figure 21 the TE is set to zero in order to isolate only the effects of CFO over the received signal.

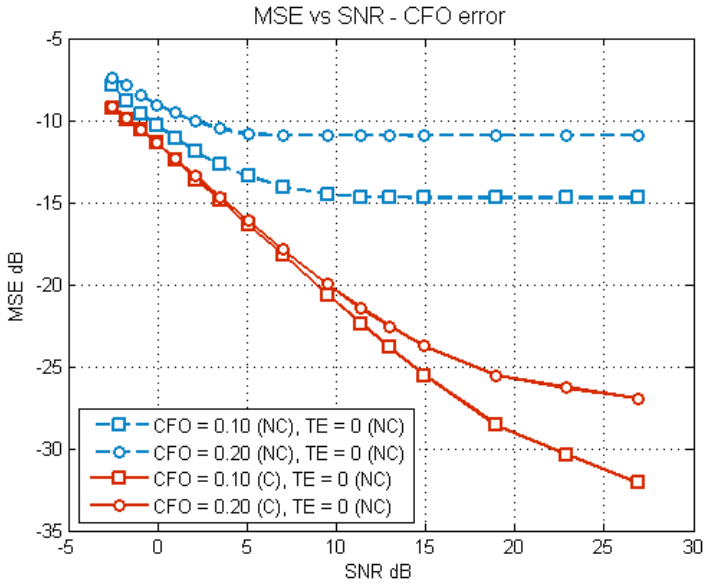

Figure 21: MSE vs. SNR, CFO compensation

From the curves, it is evident how the selected Moose algorithm is able to recover the user data symbols by applying the estimated carrier frequency offset systematically to the received symbols. The algorithm is able to perform well also at low values of SNR, in the range below 0 dB.

Figure 22 shows the performance in terms of MSE of received constellation symbols at the input of the demodulator according to different values of TE and SNR. If a TE of 1 is applied to the signal, it means that the acquisition stage output a signal with a relative drift of 1 sample w.r.t. the nominal start of frame. In the figure the CFO is set to zero in order to isolate only the effects of TE over the received signal.

From the curves, it can be seen how the selected Mengali & Morelli (M&M) algorithm is able to recover the user data symbols by applying the estimated timing error systematically to the received symbols. The algorithm is able to perform well also at low values of SNR, in the range below 0 dB. It is worth noting that M&M reduces its performance, while the value of residual timing error approaches the size of the cyclic prefix of SC-FDMA signal. This is due to the limitation in range presented by the algorithm itself.

Figure 23 finally shows the joint performance of Moose and M&M algorithms in presence of both residual CFO and TE. It is evident how the mutual cross-influence of CFO (TE) over timing (frequency) offset estimation slightly degrade the overall receiver performance, but in general the limiting factor is represented mainly by the relative amount of the CFO w.r.t. the TE, once both are estimated and compensated in the receiver chain.

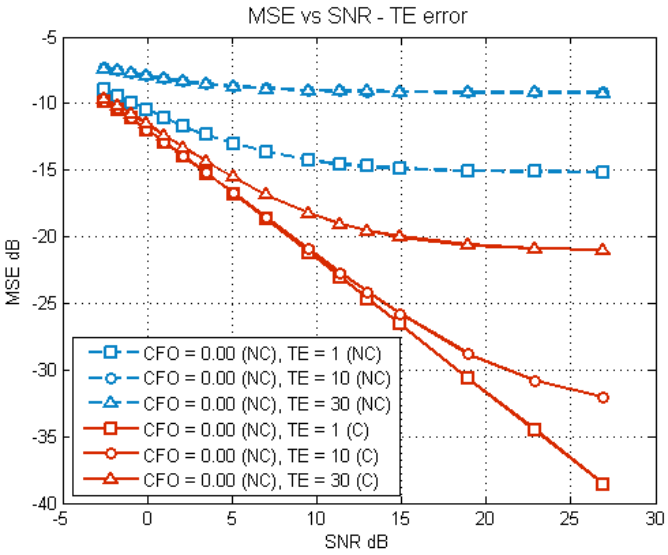

Figure 22: MSE vs. SNR, TE compensation

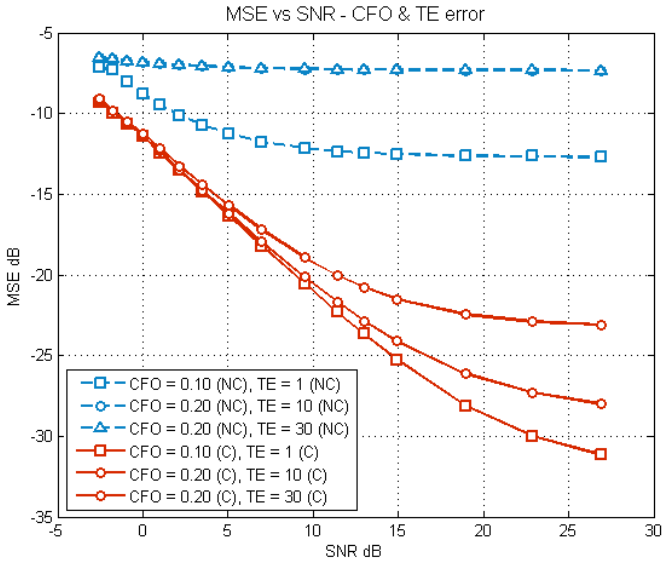

Figure 23: MSE vs. SNR, CFO and TE compensation

5.3.4.2 Power efficiency

The results for QPSK, 8-PSK and 16-QAM are presented in Figure 24, Figure 25 and Figure 26, respectively. Here, the reference SNR targets in the linear channel are 3,7 dB, 8,9 dB and 10,4 dB, respectively, for an uncoded BER of 1E-3 in the presence of the 6,1 dB amplifier gain according to the AM/AM characteristic. Data pre-distortion is shown to be an effective technique to reduce the non-linear distortion for higher order modulation, especially for 16-QAM. However, it only shows a benefit for TDMA, where the constellation warping effect is most pronounced. TDMA with 20 % roll-off expectedly shows the lowest TD in the non-linear channel followed by SC-FDMA, while OFDMA is most penalized due to the large PAPR. In addition, SC-FDMA is able to outperform TDMA with 5 % roll-off for higher constellation orders due to the residual ISI for very low roll-off factors, resulting from the truncation of the SRRCF impulse response to reduce the processing complexity and latency. Here, 16 periods of the impulse response of the filter have been considered, applying an oversampling factor of 8. The optimum OBO and minimum TD are summarized in Table 11.

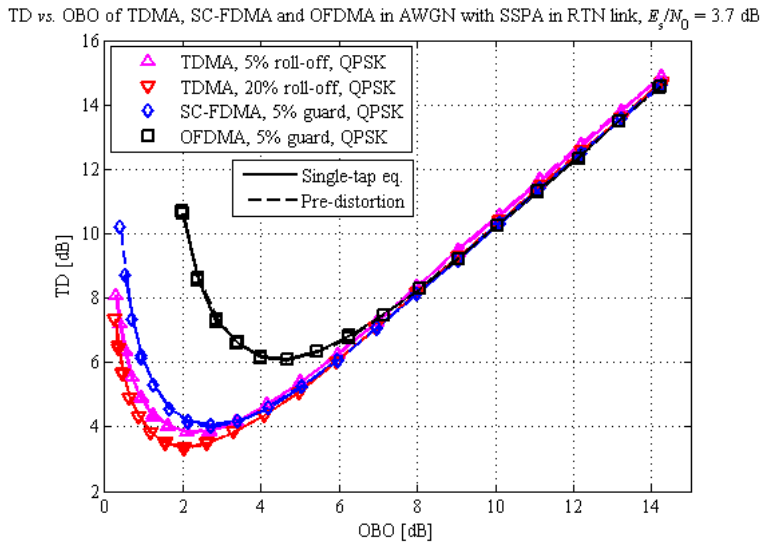

Figure 24: Total degradation as a function of OBO in TDMA, SC-FDMA and OFDMA in the return link for tighter roll-off, pre-distortion and guard band using QPSK modulation

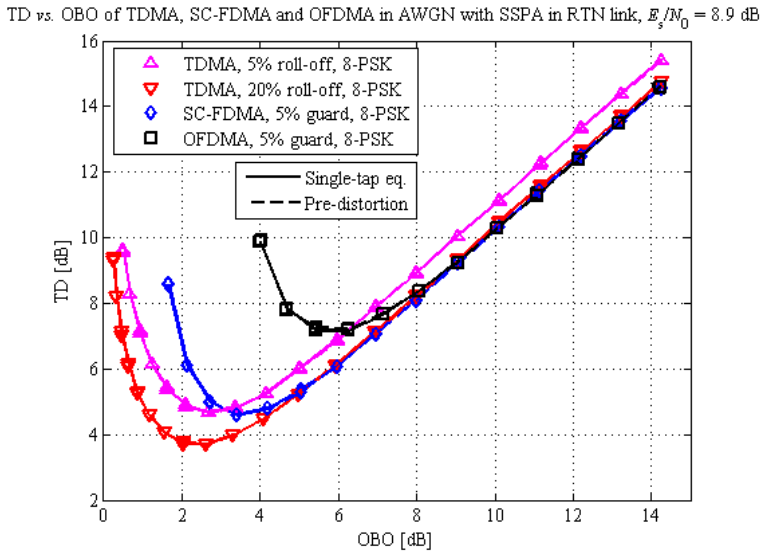

Figure 25: Total degradation as a function of OBO in TDMA, SC-FDMA and OFDMA in the return link for tighter roll-off, pre-distortion and guard band using 8-PSK modulation

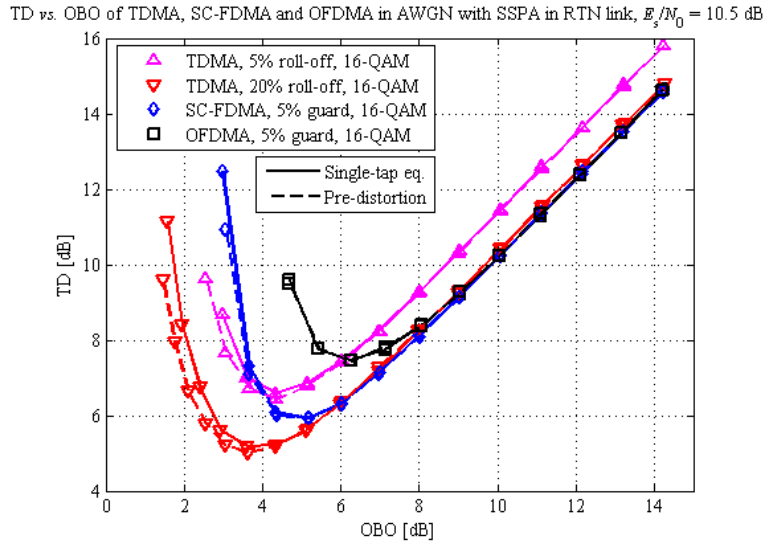

Figure 26: Total degradation as a function of OBO in TDMA, SC-FDMA and OFDMA in the return link for tighter roll-off, pre-distortion and guard band using 16-QAM modulation

Table 11: Minimum OBO and TD in SC-FDMA, TDMA and OFDMA for the modulation formats of QPSK, 8-PSK and 16-QAM (with/without pre-distortion)

Modulation and multiple access scheme	QPSK		8-PSK		16-QAM	
Minimum parameters	OBO [dB]	TD [dB]	OBO [dB]	TD [dB]	OBO [dB]	TD [dB]
SC-FDMA	2,72	4	3,4	4,6	5,19	5,94
OFDMA	4,68	6,1	5,42	7,17	6,26	7,44
TDMA with 5 % roll-off	2,1	3,85	2,7	4,67	4,34/4,35	6,43/6,58
TDMA with 20 % roll-off (benchmark)	2,03	3,33	2,03	3,71	3,64/3,6	5/5,19

5.3.4.3 Spectral efficiency

Adding the minimum TD values to the corresponding SNR targets and considering the roll-off factors and the guard bands, the spectral efficiency is shown in Figure 27 as a function of the SNR requirement. SC-FDMA demonstrates an improvement of the power efficiency of more than 1 dB as compared to state-of-the-art TDMA with 20 % roll-off, and it is able to outperform TDMA with 5 % roll-off by 0,5 dB for 16-QAM. Therefore, SC-FDMA is a promising candidate to improve the spectral efficiency of the air interface in the return link. In this setup, the improvement of the performance parameters, i.e. the spectral efficiency and SNR requirement, relative to the benchmark scheme TDMA with 20 % roll-off are summarized in Table 12. Even though the SNR requirement of SC-FDMA is slightly higher, the increase in SE yields the above mentioned more than 1 dB increase in power efficiency as compared to the benchmark.

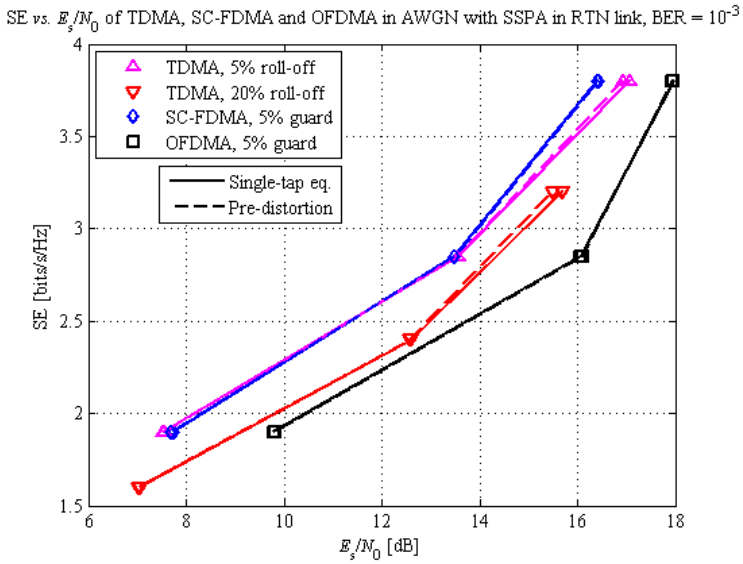

Figure 27: Spectral efficiency in TDMA, SC-FDMA and OFDMA for an SSPA in the return link for tighter roll-off, pre-distortion and guard band

Table 12: Performance parameters (SE and SNR) in SC-FDMA, TDMA and OFDMA for the modulation formats of QPSK, 8-PSK and 16-QAM (with/without pre-distortion)

Modulation and multiple access scheme	QPSK		8-PSK		16-QAM	
Performance parameters	SE [bits/s/Hz]	SNR req. [dB]	SE [bits/s/Hz]	SNR req. [dB]	SE [bits/s/Hz]	SNR req. [dB]
SC-FDMA	+18,75 %	+0,67	+18,75 %	+0,89	+18,75 %	+0,94/0,75
OFDMA	+18,75 %	+2,77	+18,75 %	+3,46	+18,75 %	+2,44/2,25
TDMA with 5 % roll-off	+18,75 %	+0,52	+18,75 %	+0,96	+18,75 %	+1,43/1,39
TDMA with 20 % roll-off (benchmark)	--	--	--	--	--	--

5.3.4.4 Complexity

The computational complexity of the waveforms of OFDMA, SC-FDMA and TDMA is compared in Table 13. For this complexity comparison, only the processing specific to the waveform is considered, i.e. pulse shaping in TDMA, IDFT and DFT operations in OFDMA and SC-FDMA. The complexity is evaluated as the number of operations required per transmitted constellation symbol. For the considered examples, it is shown that the OFDMA and SC-FDMA waveforms decrease the complexity of the transmitter and receiver by a factor approximately 3.

Table 13: Comparison of complexity per transmitted symbol of OFDMA, SC-FDMA and TDMA

	Variables definition	Number of multiplication per cell	Examples
OFDMA	N : DFT and IDFT size	$\log_2(N)$	N = 2 048 => 11 N = 8 192 => 13
SC-FDMA	N : DFT and IDFT size R: resource blocks	$\log_2(N) + \log_2(N/R)/R$	N = 2 048 => 11,01 N = 8 192 => 13,02
TDMA	Ovs : oversampling ratio L_{FIR} FIR duration in T_s	$N_{taps} = Ovs * L_{FIR}+1$	α = 5 % Ovs = 2 L_{FIR} = 20 N_{taps} = 41

5.3.5 Synthesis

In the present document, the SC-FDMA waveform has been studied in comparison with TDMA, as well as OFDMA, for application in the DVB-RCS2 satellite return link. Suitable techniques have been developed to manage the challenges in the satellite channel such as large propagation delays and non-linear transfer characteristics. GPS-based delay pre-compensation has been proposed for synchronization acquisition. This approach has been shown to increase the synchronization accuracy from the milliseconds range to the nanoseconds range, thus reducing the overhead in the transmission. For fine synchronization and tracking, the Mengali and Morelli algorithm has been selected as a suitable candidate for timing offset estimation for SC-FDMA in the return link. Also, the Moose algorithm has been proposed for frequency offset estimation.

It has been shown that the use of SC-FDMA in the DVB-RCS2 satellite return link can improve the overall spectral and power efficiency of the system at reduced computational complexity. Through optimization of the output power back-off and minimization of the total degradation, the power efficiency of the waveforms has been maximized. SC-FDMA can be used to improve the power efficiency of the air interface in the return link. A 1-dB gain is expected as compared to state-of-the-art TDMA, as well as improvement in the spectral efficiency.

Moreover, in order to facilitate the integration of satellites in LTE networks, our recommendation for the air interface in the return link is to include the following techniques:

- a GPS-based delay pre-compensation module for synchronization acquisition;
- the Mengali and Morelli algorithm for timing offset estimation in the return link;
- the Moose algorithm for frequency offset estimation in the return link;
- minimization of the total degradation through output back-off optimization resulting in the definition of an optimum amplifier setting of the user terminal for every MODCOD.

A synthesis is provided in Table 14.

Table 14: Synthesis of SC-FDMA and SC-TDM comparison (for 0 % and 5 % roll-off respectively, i.e. 18.75 % SE gain vs. TDM with 20 % roll-off)

Broadband access		SC-FDMA and SC-TDM comparison
Power Efficiency	QPSK	0,15 dB loss for SC-FDMA
	8PSK	0,07 dB gain for SC-FDMA
	16QAM	0,64 dB gain for SC-FDMA
Complexity		Number of multiplications in the equalizer divided by 3 for SC-FDMA

6 Forward Link

For further study.

7 Conclusions and Recommendations

In the present document, the SC-FDMA waveform has been studied for application in the return link of satellite networks.

The performance of this waveform was compared with SC-TDM (DVB-S2x) and TDMA (DVB-RCS2) for respectively DSNG and broadband access use cases. These comparisons were performed at the physical layer, with the same access scheme to the spectrum.

It was shown that SC-FDMA allows decreasing receiver's complexity (especially the equalizer) for comparable spectral and power efficiency performance with the SC-TDM/TDMA in both use cases.

Moreover, the use of SC-FDMA may help the integration of Satellite Communication systems with 3GPP radio access network technologies (e.g. LTE and New Radio (NR)).

Note that performance improvements can be expected with SC-FDMA in satellite return links with advanced pre-distortion techniques, which will reduce the loss induced by a lower roll-off.

Annex A: Bibliography

Casini E., Gaudenzi R. D. and Ginesi A.: "DVB-S2 modem algorithms design and performance over typical satellite channels" Int. J. Satell. Commun. Network., 22: 281-318, 2004.

Annex B:
Change History

Date	Version	Information about changes
November 2016	1.1.1	First publication of the TR after approval by TC SES at SES#90

History

Document history		
V1.1.1	July 2017	Publication